First-order transition from antiferromagnetism to ferromagnetism in $Ce(Fe_{0.96}Al_{0.04})_2$

M. A. Manekar, S. Chaudhary, M. K. Chattopadhyay, K. J. Singh, S. B. Roy,* and P. Chaddah
Low Temperature Physics Laboratory, Centre for Advanced Technology, Indore 452013, India
(Received 23 April 2001; published 22 August 2001)

Taking the pseudobinary C15 Laves phase compound $Ce(Fe_{0.96}Al_{0.04})_2$ as a paradigm for studying a ferromagnetic to antiferromagnetic phase transition, we present interesting thermomagnetic history effects in magnetotransport as well as magnetization measurements across this phase transition. A comparison is made with history effects observed across the ferromagnetic to antiferromagnetic transition in $R_{0.5}Sr_{0.5}MnO_3$ crystals.

DOI: 10.1103/PhysRevB.64.104416 PACS number(s): 75.30.Kz

The C15 Laves phase compound $CeFe_2$, with its relatively low Curie temperature ($T_C \approx 230$ K) and reduced magnetic moment ($\approx 2.3\mu_B$/f.u.) (Ref. 1) is on the verge of a magnetic instability.[2] Neutron measurements have shown the presence of antiferromagnetic (AFM) fluctuations in the ferromagnetic (FM) state of $CeFe_2$ below 100 K.[3] With a small but suitable change in electronic structure caused by doping with certain elements like Co, Al, Ru, Ir, Os, and Re at the Fe site,[4] these AFM fluctuations get stabilized into a low-temperature AFM state.[5–8]

While most recent experimental efforts are focused on understanding the cause of this magnetic instability in $CeFe_2$,[9,10] we have recently addressed the question of the exact nature of this FM-AFM transition in Ru- and Ir-doped $CeFe_2$ alloys.[11] Our results show that this is a first-order transition. The nature of the FM to AFM transition in the perovskite-type manganese oxide compounds $R_{0.5}Sr_{0.5}MnO_3$ (R=Nd,Pr,$Nd_{0.25}Sm_{0.75}$) has also been the subject of close scrutiny in recent years,[12–14] and has also been shown to be a first-order transition. The existence of metastable states, which are thought to be generic to a first-order phase transition, has been highlighted.

In this paper we report interesting thermomagnetic history dependence in the magnetization and magnetoresistance in a $Ce(Fe_{0.96}Al_{0.04})_2$ alloy, and argue that these are broader manifestations of the behavior reported earlier in the perovskite-type manganese compounds.[12–14] While the metastabilities can be partly explained by the phenomena of supercooling and superheating, we present clear signatures that the kinetics of this magnetic phase transition is hindered at low temperatures.

The details of the preparation and characterization of the polycrystalline sample can be found in Ref. 6. The samples from the same batch have been used earlier in bulk magnetic transport (Ref. 6) and neutron (Ref. 8) measurements. We have used a superconducting quantum interference device magnetometer (Quantum Design MPMS5) for measuring magnetization (M) as a function of temperature (T) and magnetic field (H). We have checked our results using scan lengths varying from 2 to 4 cm and no qualitative difference was found. We have used a commercial superconducting magnet and cryostat system (Oxford Instruments, United Kingdom) for magnetotransport measurements as a function of T and H. The resistivity was measured using a standard dc four-probe technique.

The present $Ce(Fe_{0.96}Al_{0.04})_2$ sample undergoes a paramagnetic (PM) to FM transition at around 200 K, followed by a FM to AFM transition at around 95 K (Ref. 6). We first plot in Fig. 1 M-H data at some representative T. The behavior of M at $T=100$ K is consistent with that of a soft (coercive field $\approx$100 Oe) FM state, reaching technical saturation by $H \approx 3$ kOe. With lowering of T the nature of the M-H curve changes drastically with the appearance of a hysteresis bubble. Such hysteresis,[15,16] along with the observed cubic to rhombohedral transition (Ref. 8), have been considered earlier as possible signatures of a field-induced first-order metamagnetic transition from AFM to FM in Co-doped $CeFe_2$ (Ref. 15). At $T=5$ K, we find that if the maximum field excursion is less than $|30|$ kOe, the M-H curve remains reversible in the high-field regime. In this field regime the sample remains in the AFM state. (The observed nonlinearity in the $\pm$5-kOe regime is due to parasitic weak ferromagnetism[17] leading to a canted spin state.[8,16,18]) When the applied H is increased beyond $H_M \approx 30$ kOe, M rises rapidly and upon lowering H a hysteresis is observed. The hysteresis loop, however, collapses before H is reduced to zero (coercive field $\approx$300 Oe), and reappears again in the third quadrant, giving rise to a butterflylike hysteresis loop. In Fig. 2 we present resistivity (ρ) as a function of H, at the representative temperatures $T=3$ K, 5 K, and 20 K. The sample is initially cooled to each temperature in zero field. We see the clear signature of a field-induced AFM-FM transition at a field $H_M(T)$, where the resistivity decreases sharply with increasing H. It is to be noted that in the present case of $Ce(Fe_{0.96}Al_{0.04})_2$ both FM and AFM phases are metallic, and the change in resistivity observed is not as drastic as in $R_{0.5}Sr_{0.5}MnO_3$ with R=Nd.[12] On reducing the field from well above H_M, a clear hysteresis is seen in the ρ vs H plot [see Figs. 2(a) to 2(c)]. This hysteresis is due to metastable states expected across a first-order transition where the inequality between the free energies of the two phases changes sign on a (H_M, T_N) line, but the transition to the higher entropy phase actually occurs on a (H^{**}, T^{**}) line because of superheating, and the transition to the lower entropy phase actually occurs on a (H^*, T^*) line because of supercooling.[19] We accordingly attribute this hysteresis in M vs H and in ρ vs H to the first-order nature of the field-induced FM-AFM transition. Similar hysteresis observed in the ρ-H plots of $R_{0.5}Sr_{0.5}MnO_3$ has also been attributed to the first-order nature of the phase transition.[12–14]

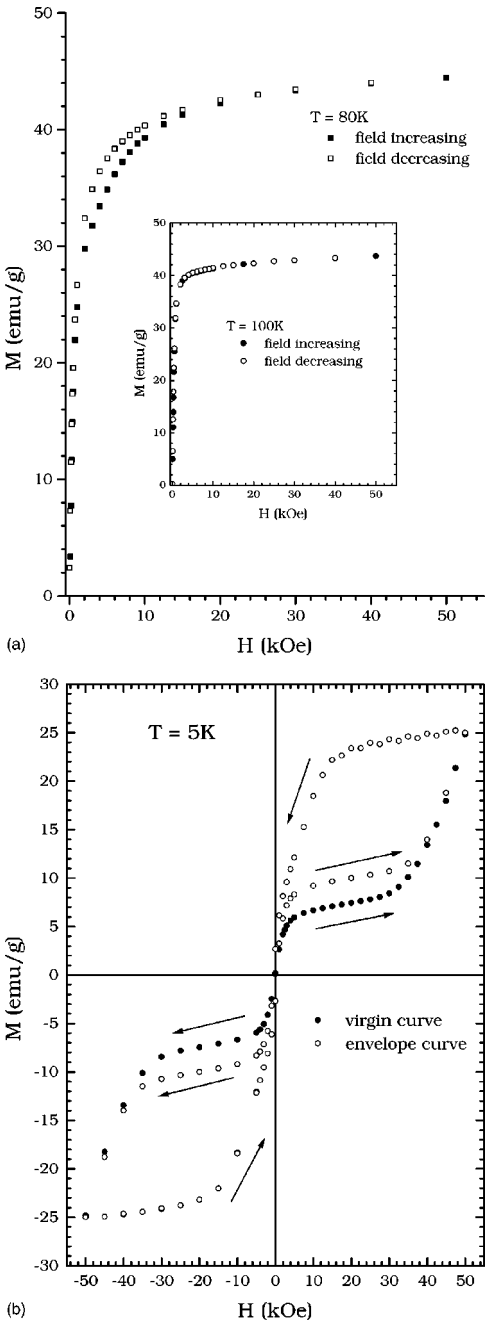

FIG. 1. M vs H plots of $Ce(Fe_{0.96}Al_{0.04})_2$ obtained after cooling in zero field (a) at $T=80$ K and 100 K and (b) at $T=5$ K. Note that at $T=5$ K the virgin M-H curve lies outside the envelope M-H curve. To confirm this anomalous nature of virgin curve we have also drawn this in the negative field direction after zero-field cooling the sample.

In this picture, the FM state continues to exist as a supercooled metastable state when H is lowered isothermally below H_M, up to the limit H^*. Between H_M and H^* fluctuations can help in nucleating droplets of the AFM state, and at H^* an infinitesimal fluctuation will drive the whole system to the stable AFM phase. Heterogeneous nucleation can thus cause a spatial distribution of the field until which supercooling is actually observed at T, resulting in the (H^*,T^*) line getting broadened into a band. Early theoretical arguments[20]

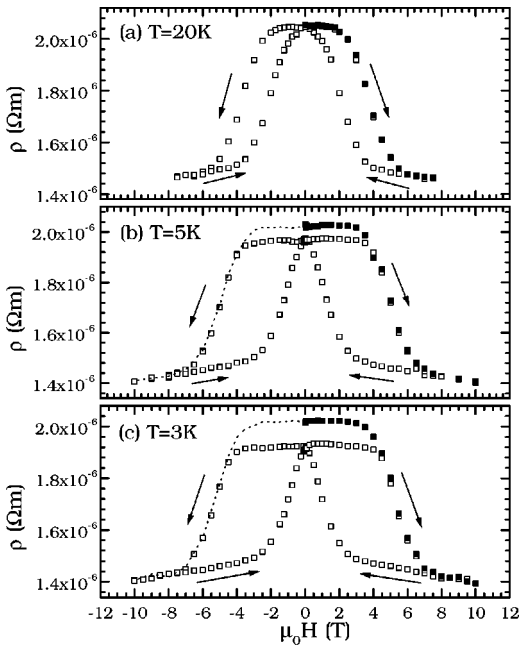

FIG. 2. R vs H plots of $Ce(Fe_{0.96}Al_{0.04})_2$ at $T=20$ K, 5 K, and 3 K. Filled squares (dashed lines) represent virgin curve drawn in the positive (negative) field direction after zero-field cooling the sample.

and recent measurements[21] also showed that a sample with disorder can have a spatial distribution of the phase-transition field H_M in a general first-order transition, hence broadening the (H_M,T_N) line into a band. This disorder would also cause the (H^*,T^*) and (H^{**},T^{**}) lines to be broadened into bands. This is depicted schematically in Fig. 3(a), and is consistent with earlier neutron-scattering observation in Al-doped $CeFe_2$ of coexisting FM and AFM phases over a finite temperature regime.[8]

We now come to some interesting features seen at very low temperatures, where the effect of thermal fluctuations is reduced. As seen in Figs. 2(b) and 2(c), when the applied field is reduced to zero from H_{max} well above H_M at $T=3$ and 5 K, the $\rho(H=0)$ lies distinctly below the initial zero-field-cooled (ZFC) $\rho(H=0)$, thus giving rise to an open hysteresis loop. This kind of open hysteresis loop has been reported earlier for single-crystal $Nd_{0.5}Sr_{0.5}MnO_3$ samples at low temperature.[12] We attribute this lower resistance to the existence of a residual metastable FM phase even at $H=0$. Is $(H=0,T=3$ K) within the (H^*,T^*) band, or can such a residual FM phase persist below the (H^*,T^*) band? We shall return to this question.

The envelope ρ-H hysteresis curves shown in Fig. 2 are obtained by reducing the field from H_{max} to zero to $-H_{max}$, and raising it back to H_{max}. We see in Fig. 2 that the virgin ρ-H curve lies outside the envelope hysteresis curve. As seen in Fig. 1, the virgin M-H curve at 5 K also lies clearly outside the envelope hysteresis curve. We argue from existing data that this anomalous feature might also be seen in $Nd_{0.5}Sr_{0.5}MnO_3$ at $T<20$ K. The reported ρ-H curve (see Figs. 2B to 2D of Ref. 12) exhibits an open hysteresis loop. In the light of our present findings, it is possible that if H were again increased from zero to 120 kOe, the forward

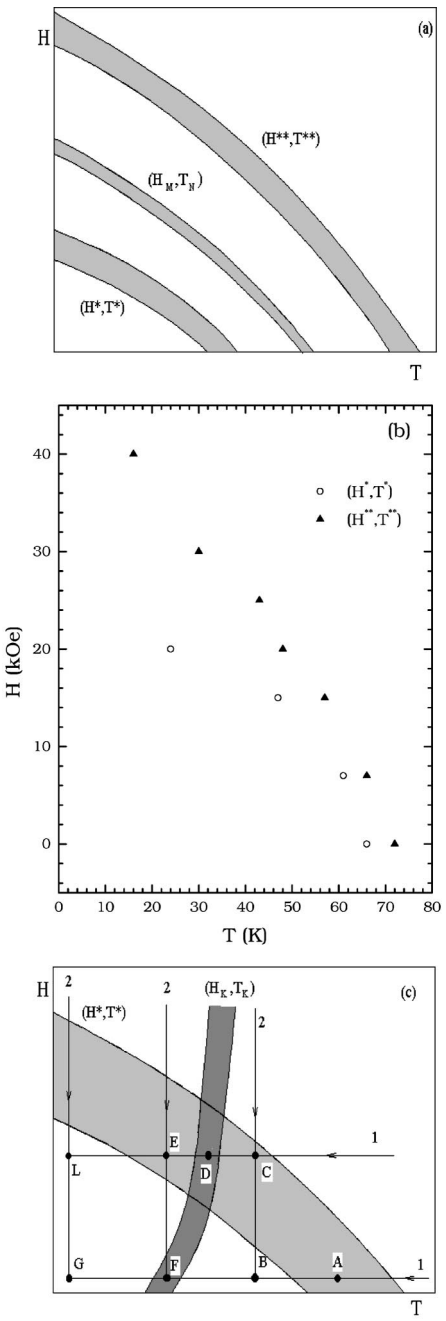

FIG. 3. (a) Schematic representation of broadened bands of phase-transition (H_M,T_N), supercooling (H^*,T^*), and superheating (H^{**},T^{**}) lines. The last two present the limits of metastability. See text for details. (b) Supercooling (H^*,T^*) and superheating (H^{**},T^{**}) points obtained from the resistivity measurements. See text for details. (c) Schematic representation of the relative position of the band (H_K,T_K) (across which the kinetics of the FM to AFM transformation is hindered) with respect to (H^*,T^*). See text for details.

leg of this envelope curve would merge with the virgin ρ-H curve only at some finite (and large) field. We consider this anomalous relation between virgin and envelope hysteresis curves at low temperatures, seen in both magnetotransport and magnetization measurements, to be significant.

We now present in Fig. 4 ρ vs T plots in fields of $H=0$, 5, 20, and 30 kOe. In each case we have cooled the sample to 5 K in zero field and then applied H at this temperature. Resistivity is then measured as the sample is warmed well into the FM state. The sample is then cooled back to 5 K in the field H, allowing a measurement of thermal hysteresis. The appearance of magnetic superzones[6,7] at the AFM-FM transition gives rise to the distinct structure observed in ρ-T. There is a marked hysteresis between the warming and cooling cycles, because the FM (or AFM) phase can be supercooled (or superheated) and exists as a metastable phase between the (H_M,T_N) line and the (H^*,T^*) line [or the (H^{**},T^{**}) line]. For $H=0$ and 5 kOe, the FM to AFM transition is completed during cooldown at $T\approx 20$ K; this indicates that $(H=0,T=5$ K) and $(H=5$ kOe,$T=5$ K) points lie below the (H^*,T^*) band and no supercooled FM phase is expected to be metastable at $H=0$ at $T=3$ K or 5 K. This is in striking contrast with the data in Fig. 2 which shows that the resistance of the AFM state is not restored when H is reduced to zero isothermally. (The ρ vs T data in $R_{0.5}Sr_{0.5}MnO_3$ shows the same contrast with the ρ-H data.[12,14]) The data in Fig. 4 also shows that for $H=20$ kOe and $H=30$ kOe the resistivity does not rise to its full AF state value on the cooling curve down to 5 K, even though the FM to AFM transformation appears to have been arrested at around 15 K. (This is again similar to the observations in Ref. 14 on the single-crystal manganite samples.) Using the data in Fig. 4 (and more such data at various other fields not shown here), we present in Fig. 3(b) the (H^*,T^*) and (H^{**},T^{**}) points for our sample. These are obtained as

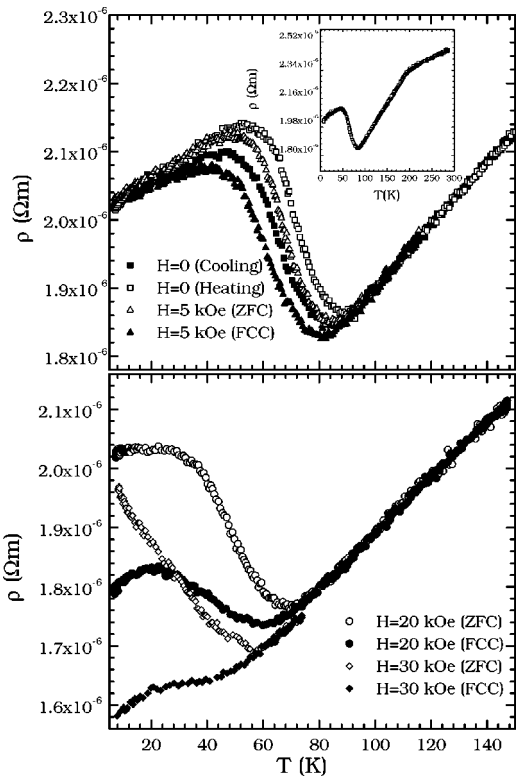

FIG. 4. ρ vs T of $Ce(Fe_{0.96}Al_{0.04})_2$ plots showing the FM-AFM transition with $H=0$, 5 kOe, 20 kOe, and 30 kOe. Inset shows the zero-field ρ-T data with both PM-FM and FM-AFM transitions.

the midpoints of the FM-AFM transition on cooling, and AFM-FM transition on heating, respectively. They thus correspond to the midpoints of the corresponding bands shown in the schematic Fig. 3(a). If superheating is not taking place, then what we have labeled as (H^{**},T^{**}) would actually correspond to (H_M,T_N).

We now summarize the unusual findings of the present study.

1. The envelope ρ-H curve at 5 K and 3 K (Fig. 2) does not return at $H=0$ to the virgin curve value of $\rho(H=0)$, while the FM to AFM transition is complete when the sample is cooled to these temperatures in low field. A similar behavior is seen from the single-crystal studies on $R_{0.5}Sr_{0.5}MnO_3$ in another first-order FM to AFM transition.[12,14]

2. The butterfly ρ-H and M-H hysteresis loops have an anomalous virgin curve at low temperatures, in that the virgin curve lies outside the envelope hysteresis curve in both measurements.

3. In the field-cooled measurement of ρ vs T at $H=20$ kOe and 30 kOe, the FM to AFM transition appears to be arrested at about 15 K even while the transformation is incomplete, and remains incomplete down to 5 K. These results are supported by the study of T dependence of M in both the zero-field-cooled and field-cooled modes.[22] Similar behavior in the resistivity studies are seen in the single-crystal studies of $R_{0.5}Sr_{0.5}MnO_3$.[14]

As a possible explanation we introduce the idea that the kinetics of the FM to AFM transition gets hindered at low T and in high H. We concentrate on the (H^*,T^*) band in Fig. 3(c), and recognize that for (H,T) values below this band the free-energy barrier separating the FM from the AFM phase has dropped to zero throughout the sample.[19] An infinitesimal fluctuation should drive any FM region to the AFM phase. But all our observations indicate that at very low T the unstable FM regions remain in the AFM phase. It is well known that at sufficiently low T the characteristic time for structural relaxation becomes larger than experimental time scales.[23] We postulate that at sufficiently low T the displacive motion of atoms involved in the structural distortion that is associated with the FM-AFM transition in $Ce(Fe_{0.96}Al_{0.04})_2$ (Ref. 8) becomes negligible on experimental time scales. The high-temperature-high-field FM phase is then frozen-in. We accordingly postulate that below a certain temperature $T_K(H)$ the kinetics of the FM-AFM transformation is hindered and arrested just like in a quenched metallic glass. (This is similar to observations at high pressures where the high-density phase cannot transform[24] to the low-density phase below a certain T_K, with T_K rising as the pressure rises.) We would depict this as a (H_K,T_K) line in the two-control-variable (H,T) space, which we broaden into a band with the same argument used to replace the other thermodynamic transition lines by a band. At temperatures below the band the freezing-in occurs throughout the sample; within the band it occurs in some regions of the sample. With this conjecture we now qualitatively explain the three unusual findings enumerated above. We use the schematic in Fig. 3(c), where paths labeled by 1 and 2 indicate cooling in constant field and lowering H at constant T, respectively. We assume that we start always with a sample that is prepared to be completely in the FM phase by warming (or increasing field) to a point well above the (H^{**},T^{**}) band.

Let us cool sequentially to points A, B, F, and G along path 1. At point A we observe FM and AFM coexistence (with FM being metastable) while at point B the entire sample is in the AFM phase. The (H_K,T_K) band has no observable effect as we cool to points F or G. This corresponds to our ρ-T data at $H=0$ or 5 kOe. Following path 1 again, we cool in higher fields to reach, sequentially, points C, D, E, and L. At C we have two-phase coexistence with FM transforming to AFM as temperature is lowered. This transformation is arrested at D, and the FM fraction is frozen-in at E and L, even though it would have kept reducing in an ergodic system. Thus we have a frozen-in FM phase at L even though it is unstable. This explains the field-cooled ρ vs T and M vs T (Ref. 22) data at fields of 20 and 30 kOe. We now follow path 2 and lower the field sequentially to points C and B. At point C we see two-phase coexistence and at point B the sample is fully AFM. This explains our M-H data and our ρ-H data at higher T. We now follow path 2 and lower the field to points E and F. At point E the FM phase is frozen-in throughout, while at F some regions of the sample are no longer kinetically arrested and transform to the AFM phase. This corresponds to our ρ-H data at 3 K and 5 K, with only partial recovery of the AFM phase even though path 1 gives a full recovery of the AFM phase. And in the ZFC state at $H=0$ we reached point F by path 1. This also explains the anomalous virgin curves because the virgin curve starts at F after path 1, then goes above the (H^{**},T^{**}) band and returns to point F by path 2 thereby retaining a fraction of the FM phase. The forward hysteresis curve now starts with coexisting FM-AFM phases unlike the virgin curve which had only an AFM phase. Because of the larger M and lower ρ of the FM phase, the forward hysteresis envelope thus lies above (or below) the virgin curve in isothermal M-H (or ρ-H) measurements. Finally, if we follow path 2 and reduce the field isothermally to reach point G, then the FM phase is frozen-in completely, and no AFM phase is recovered. This might explain the ρ-H data at 10 K reported (Ref. 14) in the $R_{0.5}Sr_{0.5}MnO_3$ single crystal with $R=Nd_{0.25}Sm_{0.75}$.

To conclude, we have observed unusual history effects in magnetization and magnetotransport measurements across the FM-AFM transition in $Ce(Fe_{0.96}Al_{0.04})_2$, and have discussed similarities with earlier single-crystal data on $R_{0.5}Sr_{0.5}MnO_3$ across another first-order FM-AFM transition. We have argued that the kinetics of this FM-AFM transition is hindered at low T. This observation may be of relevance to other first-order transitions where it is more difficult to vary two control variables; one example is the high-density amorphous water to low-density amorphous water transition which is observed with reducing pressure at 130 K, but whose kinetics appears to be arrested at 77 K.[23,25] These FM-AFM transitions can be used as paradigms to study various interesting aspects of first-order transitions such as nucleation and growth, supercooling and superheating, hindered kinetics, etc. in a relatively easy and reproducible manner.

*Corresponding author.

[1] O. Eriksson, L. Nordstrom, M.S.S. Brooks, and B. Johansson, Phys. Rev. Lett. **60**, 2523 (1988).
[2] S.B. Roy and B.R. Coles, J. Phys. F: Met. Phys. **17**, L215 (1987).
[3] L. Paolasini, P. Dervenagas, P. Vulliet, J.P. Sanchez, G.P. Lander, A. Hiess, A. Panchula, and P. Canfield, Phys. Rev. B **58**, 12 117 (1998).
[4] P.K. Khowash, Phys. Rev. B **43**, 6170 (1991).
[5] A. K. Rastogi and A. P. Murani, in *Theoretical and Experimental Aspects of Valence Fluctuations and Heavy Fermions*, edited by L. C. Gupta and S. K. Malik (Plenum New York, 1987), p. 437.
[6] S.B. Roy and B.R. Coles, J. Phys.: Condens. Matter **1**, 419 (1989).
[7] S.B. Roy and B.R. Coles, Phys. Rev. B **39**, 9360 (1989).
[8] S.J. Kennedy and B.R. Coles, J. Phys.: Condens. Matter **2**, 1213 (1990).
[9] J. Chaboy, C. Piquer, L.M. Garcia, and F. Bartolome, Phys. Rev. B **62**, 468 (2000).
[10] R.J. Lange, I.R. Fisher, P.C. Canfield, V.P. Antropov, S.J. Lee, B.N. Harmon, and D.W. Lynch, Phys. Rev. B **62**, 7084 (2000).
[11] M. Manekar, S.B. Roy, and P. Chaddah, J. Phys.: Condens. Matter **12**, L409 (2000); **12**, 9645 (2000).
[12] H. Kuwahara, Y. Tomioka, A. Asamitsu, Y. Moritomo, and Y. Tokura, Science **270**, 961 (1995).
[13] Y. Tomioka, A. Asamitsu, Y. Moritomo, H. Kuwahara, and Y. Tokura, Phys. Rev. Lett. **74**, 5108 (1995).
[14] Y. Tokura, H. Kuwahara, Y. Moritomo, Y. Tomioka, and A. Asamitsu, Phys. Rev. Lett. **76**, 3184 (1996).
[15] N. Ali and X. Zhang, J. Phys.: Condens. Matter **4**, L351 (1992).
[16] H. Wada, M. Nishigori, and M. Shiga, J. Phys. Soc. Jpn. **62**, 1337 (1993); H. Fukuda, H. Fujii, H. Kamura, Y. Hasegawa, T. Ekino, N. Kikugawa, T. Suzuki, and T. Fujita, Phys. Rev. B **63**, 054405 (2001).
[17] S. Chikazumi, *Physics of Ferromagnetism* (Clarendon Press, Oxford, 1997).
[18] H.P. Kunkel, X.Z. Zhou, P.A. Stampe, J.A. Cowen, and G. Williams, Phys. Rev. B **53**, 15 099 (1996).
[19] P. M. Chaikin and T. C. Lubensky, *Principles of Condensed Matter Physics* (Cambridge University Press, Cambridge, England, 1995), Chap. 4; P. Chaddah and S.B. Roy, Phys. Rev. B **60**, 11 926 (1999).
[20] Y. Imry and M. Wortis, Phys. Rev. B **19**, 3580 (1979).
[21] A. Soibel, E. Zeldov, M. Rappaport, Y. Myasoedov, T. Tamegai, S. Ooi, M. Konczykowski, and V.B. Geshkenbein, Nature (London) **406**, 283 (2000).
[22] M.A. Manekar, S. Chaudhary, M.K. Chattopadhyay, K.J. Singh, S.B. Roy, and P. Chaddah, cond-mat/0012472 (unpublished).
[23] P. G. Debenedetti, *Metastable Liquids* (Princeton University Press, Princeton, NJ, 1996), Chap. 4.
[24] S.M. Sharma and S.K. Sikka, Prog. Mater. Sci. **40**, 1 (1996).
[25] O. Mishima and E.H. Stanley, Nature (London) **396**, 329 (1998).